



Antiferromagnetism and superconductivity: Determination of the Cu spin–spin relaxation time T_2 and the spin–lattice relaxation time T_1 in $\text{Gd}_{1.5}\text{Ce}_{0.5}\text{Sr}_2\text{Cu}_2\text{RuO}_{10}$

H.A. Blackstead^{a,*}, W.B. Yelon^b, M.P. Smylie^a

^a Physics Department, University of Notre Dame, Notre Dame, IN 46556, USA

^b Missouri University of Science and Technology, Materials Research Center and Department of Chemistry, Rolla, MO 65401, USA

ARTICLE INFO

Article history:

Received 4 June 2009

Accepted 12 June 2009 by F. De la Cruz

Available online 23 June 2009

PACS:

74.20.Mn

74.25.Ha

74.70.Pq

76.50.+g

Keywords:

A. Superconductivity

A. Antiferromagnetism

ABSTRACT

$\text{Gd}_{1.5}\text{Ce}_{0.5}\text{Sr}_2\text{Cu}_2\text{RuO}_{10}$ exhibits antiferromagnetic resonance at 23.9 GHz for applied fields less than 1000 Oe with a spin–spin relaxation time T_2 of approximately 0.45 ns, and with a spin–lattice relaxation time T_1 of at least 320 μs . Since in the homologue, $\text{Eu}_{1.5}\text{Ce}_{0.5}\text{Sr}_2\text{Cu}_2\text{RuO}_{10}$, the Ru atoms evidently fail to exhibit magnetic order, the antiferromagnetic resonance must arise from the cuprate planes. In other homologues, the cuprate planes are known to order ferromagnetically and are stacked in an antiferromagnetic configuration. The large value of T_1 suggests that phonon mediation plays no role in high temperature superconductivity. In addition, the presence of ferromagnetic cuprate planes is inconsistent with spin-fluctuation models of high temperature superconductivity.

© 2009 Elsevier Ltd. All rights reserved.

1. Introduction

The origin of the anomalous magnetization observed in field-cooled measurements of the superconducting ruthenocuprates such as $\text{Gd}_{1.5}\text{Ce}_{0.5}\text{Sr}_2\text{Cu}_2\text{RuO}_{10}$ (O10) has been widely attributed to ferromagnetic order, or canted antiferromagnetism, of the Ru in the RuO_2 layer [1]. In the closely related O8 compounds such as $\text{GdSr}_2\text{RuCu}_2\text{O}_8$, the anomalous magnetization has been attributed to a ferromagnetic component on the Ru sites, but several neutron scattering studies have failed to show any evidence for such an origin, reporting, instead, simple antiferromagnetic Ru order. The situation in the O10 compounds is further complicated by the body centered unit cell which leads to a very long c -axis. Fig. 1 shows that antiferromagnetic superexchange interactions of the Ru spins in the O10 compounds are geometrically frustrated by the presence of the fluorite $\{(\text{Gd}, \text{Ce})_2\text{O}_7\}$ block which introduces a shift of $(\mathbf{a}/2, \mathbf{a}/2)$ in the layer stacking. Neutron diffraction measurements by Kuz'micheva et al. [2] failed to detect magnetic order in $\text{Nd}_{1.4}\text{Ce}_{0.6}\text{Sr}_2\text{Cu}_2\text{RuO}_{10}$ and more recent extensive measurements by Lynn [3] et al. failed to find Ru antiferromagnetic order and also specifically excluded ferromagnetic order of the Ru in

$\text{Eu}_{1.5}\text{Ce}_{0.5}\text{Sr}_2\text{Cu}_2\text{RuO}_{10}$ in the temperature range of interest here. Since the Y homologue with Nb replacing Ru also exhibits similar magnetic behavior [4], and closely related $\text{YSr}_2\text{Cu}_2\text{NbO}_8$ does as well [5], attention is necessarily focused on the cuprate (CuO_2) planes. Neutron diffraction studies [6,7] have shown these to be magnetically ordered in the closely related material $\text{YSr}_2\text{Cu}_2\text{RuO}_8$.

As it happens, the magnon energy gap of the ordered Cu spins in the ruthenocuprates is sufficiently small that antiferromagnetic resonance is easily detected at conventional microwave frequencies. In some cases, antiferromagnetic resonance can also be observed in cuprates [8]. In the following, we present the results of such measurements as a function of the rf power level at a temperature of 100 K, substantially above the ~ 40 K superconducting transition temperature. These data show that the cuprate plane antiferromagnetic mode is surprisingly easy to saturate, indicating a long spin–lattice relaxation time, T_1 . In addition, the spin–spin relaxation time T_2 is quite short, leading to a broad field-dependent response. The Gd spins exhibit paramagnetic resonance which shows no saturation effects in the range of rf power levels employed. The Gd resonance is superimposed on the broad Cu response, and is used to calibrate the intensity of Cu resonance.

2. Experimental details

The procedure for sample preparation is described elsewhere [9], and follows conventional solid state reaction procedures. The microwave spectrometer employed has novel features

* Corresponding address: Physics Department, University of Notre Dame, 225 Nieuwand Science Hall, 46556 Notre Dame, IN, USA. Tel.: +574 631 7078.

E-mail address: blackstd@nd.edu (H.A. Blackstead).

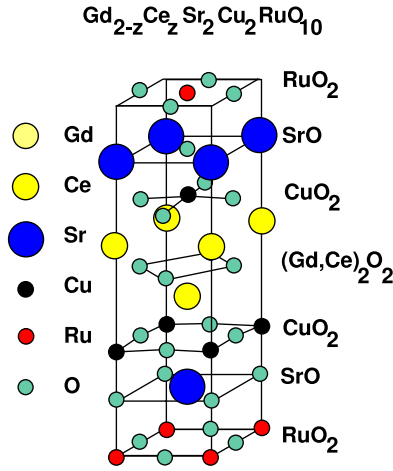


Fig. 1. Schematic structure of $\text{Gd}_{1.5}\text{Ce}_{0.5}\text{Sr}_2\text{Cu}_2\text{RuO}_{10}$, here 1/2 of the unit cell is shown. Replacement of Gd in $\text{GdSr}_2\text{Cu}_2\text{RuO}_8$ with the fluorite block $(\text{Gd}, \text{Ce})_2\text{O}_2$ results in a similar structure in which the antiferromagnetic Ru superexchange is frustrated, and it fails to exhibit long-ranged order. The Cu order ferromagnetically and are stacked antiferromagnetically. The Cu superexchange interactions across the RuO_2 and SrO layers are not frustrated for this configuration.

which were used to advantage in these measurements. One of these features is that the spectrometer (see Fig. 2) does not utilize magnetic field modulation. Field modulation is employed with a lock-in amplifier to extract the derivative of the lineshape as a function of the applied field. For resonances with large linewidths, very small signals would result. Since we did not use this technique, it was possible to measure signals with very large linewidths. In addition, the power reflected from the sample-bearing cavity was amplified using a low-noise solid state amplifier with a gain of nearly 30 db. An attenuator following the klystron source was used to control the power level incident on the cavity. Another attenuator placed after a directional coupler, and before the amplifier, was adjusted to compensate for changes in incident power levels. Thus, the point-contact diode detector, except for the lowest power levels utilized, was driven by a nearly constant power level. This is of some importance, since such detectors have a square-law response, and a constant power level biases them to a reproducible sensitivity. Additional circuitry (not shown) was employed to “lock” the klystron frequency to the resonant frequency of the sample-bearing TE_{101} rectangular cavity [10]. This feature ensures that only changes in χ'' will be detected. The polycrystalline sample was mounted in the center of the bottom of the cavity, using a small quantity of silicone grease. For the data reported here, the dc magnetic field H was applied perpendicular to the very uniform cavity magnetic field (H_{rf}), in the usual configuration for magnetic resonance. Similar Cu signals were detected with $H \parallel H_{rf}$, but in that case the paramagnetic Gd resonance was very small, and it was not useful as a calibration signal.

3. Analysis of the data

The resonant response (aside from an amplitude including H_{rf}^2) was characterized using a form given by Dyson [11,12] for conducting materials, including the term in the denominator which involves the rf field intensity and leads to saturation at high rf power levels:

$$y(H) = \frac{1 + \alpha\gamma T_2(H - H_0)}{1 + \gamma^2 T_2^2(H - H_0)^2 + \gamma^2 T_1 T_2 H_{rf}^2}. \quad (1)$$

Here γ is the gyromagnetic ratio given by $\gamma = (g\mu_B)/h$, T_1 and T_2 are the spin–lattice and spin–spin relaxation times, respectively,

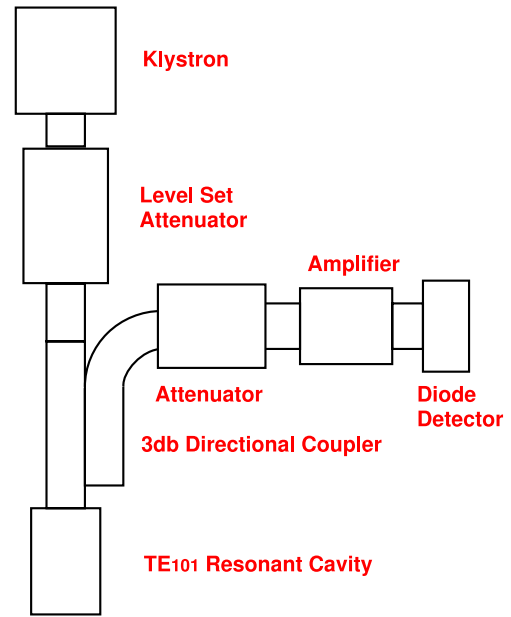


Fig. 2. Simplified block diagram of the K-band microwave spectrometer. The directional coupler serves to separate the incident power from the power reflected from the resonant cavity. The power level was set with the attenuator in series with the klystron source, and an approximately constant power level was provided to the amplifier by adjusting the compensating attenuator following the directional coupler.

and $\alpha = 0.63$ is a parameter of the fit to the data expressing the line-asymmetry. The signal resulting from an experiment is proportional to $H_{rf}^2 y(H)$; saturation of the response occurs for large rf fields. At resonance, the lineshape $y(H = H_0)$ is:

$$y(H = H_0) = \frac{1}{1 + \gamma^2 T_1 T_2 H_{rf}^2}. \quad (2)$$

Note that $y(H)$ is maximum for $H > H_0$, a consequence of the asymmetry of the Dysonian lineshape function. Because the Gd relaxation times are both small, the Gd paramagnetic response does not saturate. It follows that if $\gamma^2 T_1 T_2 H_{rf}^2 > 1$, the signal intensity, normalized by the Gd signal, will be substantially reduced at high power levels [13]. Usually in metals, this condition is difficult to satisfy owing to the small sizes of both T_1 and T_2 . For sufficiently low power levels the resonance signal is not a function of T_1 , and T_2 is independently determined by the linewidth, see Figs. 3 and 4. As a function of attenuator setting (in db), $H_{rf} = H_{rf0} 10^{-\frac{db}{20}}$. The product $T_1 H_{rf0}^2$ was found by fitting signal intensities as a function of this parameter, see Fig. 5. An upper limit for H_{rf0} was determined from the cavity radiation quality factor “Q”, the input rf power level, and the cavity and waveguide dimensions [14,15]. The result of this evaluation is that $(H_{rf0}) \leq 2.0$ Oe. It follows from the results shown in Fig. 5 and the estimated value for H_{rf} that $T_1 \geq 320 \mu\text{s}$, while from the linewidth, T_2 was found to be ~ 0.45 ns.

4. Discussion

We have recently shown in a sequence of materials which contain Ru^{4+} or Ru^{5+} in octahedral coordination with six oxygen, that the Ru are esr silent in both paramagnetic and magnetically ordered configurations [16]. These results exclude Ru as the source of the resonance discussed here. The results of the recent neutron diffraction experiments on two materials, $\text{Eu}_{1.5}\text{Ce}_{0.5}\text{Sr}_2\text{Cu}_2\text{RuO}_{10}$ and $\text{Y}_{1.5}\text{Ce}_{0.5}\text{Sr}_2\text{Cu}_2\text{NbO}_{10}$ are of critical importance to the interpretation of the results of the experiments presented here.

Download English Version:

<https://daneshyari.com/en/article/1594476>

Download Persian Version:

<https://daneshyari.com/article/1594476>

[Daneshyari.com](https://daneshyari.com)